*Environ. Sci. Technol.* **1999**, *33,* 625−630

# Transformation of Pb(II) from Cerrusite to Chloropyromorphite in the Presence of Hydroxyapatite under Varying Conditions of pH

PENGCHU ZHANG*

*Sandia National Laboratories, Geochemistry Department, MS 0750, Albuquerque, New Mexico 87185*

JAMES A. RYAN

*National Risk Management Research Laboratory, U.S. Environmental Protection Agency, 5995 Center Hill Avenue, Cincinnati, Ohio 45224*

The soluble Pb concentration and formation of chloropyromorphite [$Pb_5(PO_4)_3Cl$] were monitored during the reaction of cerrusite ($PbCO_3$), a highly bioavailable soil Pb species, and hydroxyapatite [$Ca_5(PO_4)_3OH$] at various P/Pb molar ratios under constant and dynamic pH conditions. Under pH-constant systems at pH 4 and below, the dissolution rates of both cerrusite and apatite were rapid, and complete conversion of cerrusite to chloropyromorphite occurred within 60 min when the amount of phosphate added via apatite was stoichiometrically equal to that needed to transform all added Pb into chloropyromorphite. The concentration of soluble Pb depended upon the solubility of chloropyromorphite. The dissolution rates of apatite and cerrusite decreased with increasing pH, and the transformation was incomplete at pH 5 and above in the 60-min reaction period. The soluble Pb level, therefore, was determined by the solubility of cerrusite. In the pH-dynamic system, which simulated the gastrointestinal tract (GI tract), a complete transformation of Pb from cerrusite to chloropyromorphite was achieved due to the complete dissolution of apatite and cerrusite at the initial low pH. In both the constant and dynamic pH systems XRD analysis indicated that chloropyromorphite was the exclusive reaction product. The differences in transformation rate and the Pb solubility between the constant and dynamic pH systems indicate the significance of kinetics in controlling the bioavailability of Pb and the potential for the reaction to occur during ingestion.

## Introduction

Cost-effectiveness and environmental friendliness have made the addition of phosphate minerals to Pb-contaminated soil a promising technology to remediate Pb-contaminated soils. The recent research results have demonstrated the reduction in soluble Pb levels of soil solutions by mixing phosphate minerals with Pb-contaminated soils (*1*−*9*) and the formation of pyromorphite in aqueous Pb solution on exchange resin surface and from geothite-adsorbed Pb by reaction with hydroxyapatite (*2, 3, 8, 10*). The existence of pyromorphite in the contaminated soils, road-side soils, and minewastes has been documented (*11, 12*). Furthermore, pyromorphite formation in contaminated soils amended with phosphate and hydroxyapatite (*9, 13, 14*) have also been reported.

It is generally agreed that the risks of soil Pb movement into groundwater aquifers (mobility) and of being absorbed by plants (phytoavailability), animals, and/or human beings (bioavailability) are influenced by the Pb species as well as the total Pb content in the soil. The reported soil Pb bioaccessibility results were consistent with Pb speciation results (*15, 16*). For example, a greater fraction of bioaccessible Pb was obtained in the soil containing more soluble Pb phases such as lead oxide and cerrusite than the soil containing galena, anglesite, lead phosphate, and encapsulated Pb phases (*17, 18*). Solubility, therefore, is used in reference to the stability of a specific Pb species. However, solubility is a thermodynamic parameter and is only defined when the reaction reaches equilibrium. In a dynamic system like soil, the kinetics of a reaction must be considered in order to determine the possibility and the extent of a reaction occurring under a given condition and time scale. For example, in a kinetic study, the significant difference in the amount of Pb leached from soil and waste by acid was attributed to differences in dissolution rates of the two types of Pb solid phases (*19*). Therefore, in addition to the solubility, the dissolution rates of a solid Pb-bearing form and the possible reaction products should be considered when evaluating the stability of the Pb form reacting in a dynamic system.

An accepted paradigm is that the free metal species, e.g., the bare metal cation ($M^{n+}$), is the most bioactive and the most toxic. The formation of ion pairs, complex ions, polymers, and microparticulates (e.g., colloidal iron oxide or humic substances) of a bare metal cation will alter its potential for uptake by living organisms and toxicity (*20*). The free Pb ion concentration should be the critical parameter to monitor in soil solution or gastrointestinal fluid when evaluating the bioavailability of soil Pb species. Thermodynamically, in the aqueous suspension of a group of Pb minerals, the one with the least solubility will determine the soluble Pb level as long as there is a source of ligand to precipitate the soluble Pb as the least soluble Pb mineral. Phosphate minerals, when added to Pb-contaminated soils in sufficient quantity, establish a phosphate source that can maintain the soluble phosphate at a level sufficient to precipitate the dissolved Pb as pyromorphite. Thus, the soluble Pb level will be controlled by the least soluble pyromorphite instead of the original soil Pb species. However, when sufficient phosphate mineral to stoichiometrically precipitate the total soil Pb into pyromorphite has been added, the soluble Pb level may not necessarily be controlled by pyromorphite if the dissolution rate of the added phosphate mineral is not sufficient to deliver the soluble phosphate needed to precipitate the dissolved Pb. Thus, kinetic concerns may become more important than thermodynamics in a dynamic system like soil. This kinetic concern becomes critical if the added phosphate minerals and soil Pb are simultaneously placed into a living organism.

The dominant mechanism of pyromorphite formation in the Pb−P−$H_2O$ system has been reported as precipitation of soluble lead and phosphate (*1, 8, 21*), although substitution of Pb for Ca in apatite may be possible (*12*). The formation of pyromorphite from soluble phosphate and Pb has been found to be a rapid process; soluble Pb can be depleted from solution within a few seconds if a stoichiometric amount of phosphate is provided and the system is well mixed (*1, 2*). Thus, the soluble Pb concentration in the aqueous system

* Corresponding author telephone: (505)844-2669; fax: (505)844-7354; e-mail: PZHANG@SANDIA.GOV.

10.1021/es980268e CCC: $18.00 
Published on Web 01/06/1999

containing apatite and Pb-bearing solids will be determined by the dissolution rate of apatite and the overall Pb release rate (desorption, dissociation, and dissolution) of the Pb species. Therefore, knowledge of reaction kinetics in the Pb-bearing solids and phosphate mineral provides additional information needed in the evaluation of the technology of immobilization of soil Pb and offers the basis to improve the technology.

To demonstrate this, a series of kinetic experiments were conducted in systems containing hydroxyapatite and cerrusite to determine the effects of dissolution rates of apatite and cerrusite on (i) the soluble Pb level during the reactions and (ii) the formation of pyromorphite. Cerrusite is a secondary Pb mineral commonly found in soils (*22*, *23*). It is also a weathering product of other secondary Pb minerals such as anglesite ($PbSO_4$) under appropriate condition of $CO_2$ partial pressure or activity (*24*). Cerrusite is not stable and dissolves under acid pH conditions, e.g., acidified rain (*25*). It has been demonstrated that the bioavailability of lead carbonate was higher than other soil Pb species such as anglesite and Fe−Mn-associated Pb. Furthermore, the Pb content in the plants grown on the Pb-contaminated soils was primarily associated with soil lead carbonate content rather than the total soil Pb concentrations (*26*, *27*). Thus, cerrusite can be an important mineral form of Pb in controlling the soil Pb mobility and reactivity; it can also be a highly bioavailable form of soil Pb.

## Materials and Methods

**Materials**. Analytical reagent lead carbonate ($PbCO_3$) used in this study was from Fisher Scientific. Although an amorphous morphology was observed under a scanning electronic microscope, the powder X-ray diffraction analysis illustrated a characteristic pattern of crystalline cerrusite mineral. The mineral had a specific surface area of 2.61 $m^2$ $g^{-1}$ measured by BET nitrogen absorption. The synthetic hydroxyapatite [$Ca_5(PO_4)_3OH$] used was obtained from Bio-Rad and had a specific surface area of 67.3 $m^2$ $g^{-1}$, and the P/Ca molar ratio was 1.62, which is comparable to the ideal ratio of 1.67 for hydroxyapatite.

**Dissolution of Cerrusite and Apatite.** Determination of dissolution rates for cerrusite and hydroxyapatite were conducted in a 1.1-L glass beaker placed in a water bath at 37 °C, analogous to that of human body. A 1.0-L solution of 0.001 M NaCl and 0.1 M $NaNO_3$ was measured into the beaker and adjusted to the designated pH with 0.1 M $HNO_3$ or 0.1 M NaOH. After cerrusite or apatite was added, the solution pH was maintained by an autotitrator (Mettler, DL70ES). The suspension was continuously stirred with a plastic paddle and sampled after 1, 3, 5, 10, 15, 25, 40, 60, and 120 min of reaction. Samples were immediately filtered through a 0.2-$\mu$m filter, and the filtrate was acidified and refrigerated until analyzed. The concentrations of Pb, Ca, and $PO_4$ in the solution as a function of time were used to determine the dissolution rate for cerrusite and hydroxyapatite.

**Reactions between Cerrusite and Apatite.** The effects of reaction kinetics of cerrusite and apatite on the transformation of Pb from cerrusite into pyromorphite and on the soluble Pb levels during the reactions were determined in the systems in which the pH was maintained constant or the pH was adjusted with reaction time. The later was to simulate a gastric situation in terms of pH range and time scale.

The average pediatric gastric pH was reported to be 1.7−1.8 in a fasting stomach (*18*). Following ingestion of food, the pH rises to 4−6 and then returns to basal values within 2 h. A child's stomach empties in about 60 min (*18*). About 20 min after feeding, stomach emptying starts, and the chyme enters the small intestine where the pH values reach 7 and Pb absorption occurs. Accordingly, a pH range of 2−7 was selected to simulate the GI tract pH values. In addition to the measurements conducted in constant pH suspensions (pH-constant study), a reaction was carried out in the suspension in which the pH was adjusted vs time from pH 2 to pH 7 within 20 min (pH-dynamic study). The pH-dynamic study allows the determination of the potential transformation rate of Pb from cerrusite to pyromorphite under simulated GI tract pH conditions, assuming that cerrusite and apatite were ingested simultaneously.

**pH-Constant Study**. To measure the reactions between cerrusite and hydroxyapatite, 1.0 g of cerrusite was mixed with apatite at three elemental ratios of P/Pb (3/5, 6/5, and 9/5) providing 1, 2, and 3 times the stoichiometric P/Pb ratio of chloropyromorphite, [$Pb_5(PO_4)_3Cl$]. The cerrusite and apatite mixture was added into 1.0 L of 0.001 M NaCl and 0.1 M $NaNO_3$ solution at a predetermined pH. The pH of the suspension was maintained by the autotitrator, and the suspension was sampled periodically while the system was continuously stirred. Sampled suspension was filtered through a 0.2-$\mu$m membrane, and the filtrate was analyzed for soluble $PO_4$, Pb, and Ca. At the end of a 60-min reaction, a sample of the suspension was filtered with a 0.45-$\mu$m membrane, and the solid was collected and dried for XRD analysis. From each of the P/Pb ratios, the reaction at pH 6 was allowed to continue for 48 h before the solid was collected to observe the reaction over a relatively long period.

**pH-Dynamic Study**. In a separate experiment, cerrusite was reacted with apatite (0.40 g of apatite/1.00 g of cerrusite, P/Pb = 3.2/5) while the solution pH was adjusted in increments of 1 pH unit from pH 2 to pH 7 over a 20-min time interval and then maintained at pH 7 until the end of the 60-min reaction. The suspension was sampled twice at each pH of 2, 3, 4, 5, 6, and 7. One sample was collected 1 min after the pH was established, and the second sample was taken before the pH was adjusted to next level. Sample suspension was filtered through a 0.2-$\mu$m membrane, and the soluble species concentrations of $PO_4$, Ca, and Pb were determined to assess mineral dissolution rate and Pb bioaccessibility during the reaction as well as the transformation rate of Pb from cerrusite into pyromorphite. A separate experiment with the same procedure was conducted with 1.00 g of cerrusite but without the addition of hydroxyapatite to serve as an experimental control.

**Analytical Procedures.** An inductively coupled plasma spectrophotometer (ICP, Trace 61 E, Thermal Jarrell Ash) was employed to analyze $PO_4$, Ca, and Pb concentrations. The detection limit for these three elements was 2 $\mu$g $L^{-1}$. The U.S. EPA Water Supply Performance Evaluation Study solution (WS033) was used to calibrate and verify the analytical standard solutions used for ICP analysis. Experimental blanks, standards, and spiked samples were used for analytical quality control. Solution and suspension pH was measured using a glass pH electrode that was connected to the Mettler titrator. With this setup, the variation of pH could be maintained within 0.01 pH unit.

A X-ray diffractionmeter (Scintag, XDS 2000) with Cu-K$\alpha$ radiation at 35 kV and 30 mA was used. Solids used for XRD analysis were air-dried, crushed, and mounted on a glass sample holder. XRD patterns were collected using a step-scanning rate of 0.04° 2$\theta$/s.

To quantify the mineral composition of the reacted solid collected at the end of the reaction, a portion (0.010 g) of dried solid was dissolved in 100.0 mL of a 10% $HNO_3$ and analyzed for $PO_4$, Pb, and Ca contents using ICP. As no Ca mineral other than the added apatite was found in the solid by XRD, the Ca content in the solid was used to compute the amount of undissolved hydroxyapatite. The amount of $PO_4$ in the solids was attributed to both apatite and the newly formed chloropyromorphite. Lead in the solid was attributed to both cerrusite and chloropyromorphite. From a mass balance analysis, the percentage of cerrusite-Pb transformed

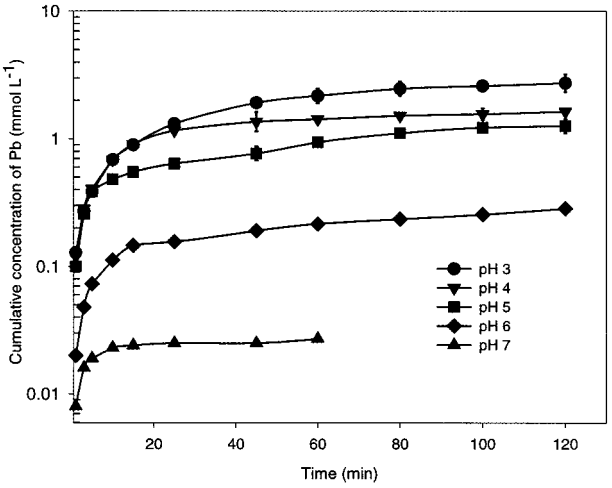


**FIGURE 1. Effect of pH on dissolution rate of cerrusite as a function of time; initial cerrusite = 1.00 g, $NaNO_3$ = 0.100 M, and NaCl = 0.001 M.**

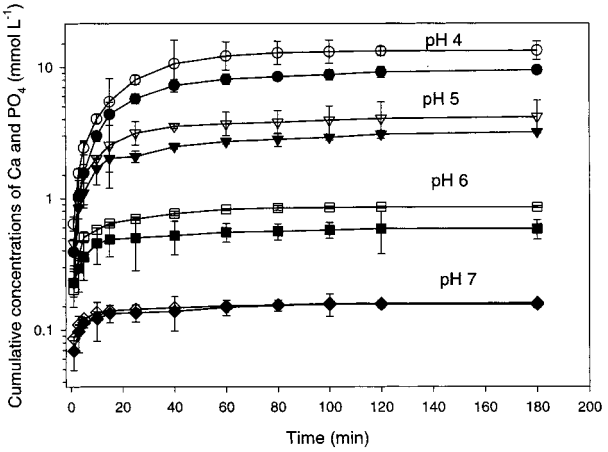


**FIGURE 2. Dissolution of hydroxyapatite as a function of time and pH. The filled and unfilled symbols represent the phosphate and calcium concentrations, respectively.**

into pyromorphite-Pb was estimated. The XRD analysis results were used to evaluate and confirm the assumption of only the three minerals (cerrusite, chloropyromorphite, and apatite) in the collected solids.

## Results and Discussion

**Dissolution of Cerrusite and Hydroxyapatite.** The dissolution of cerrusite expressed as the function of soluble Pb concentration vs time at each of the five pH values illustrates that the dissolution process is pH-dependent (Figure 1). Dissolution did not reach a steady state during the 120-min reaction period. Because of experimental difficulty in maintaining a stable pH 2 in the presence of cerrusite, no measurements were made at pH 2.

There was no attempt in this study to develop a comprehensive dissolution rate equation for cerrusite because of the difficulty in accurately determining the activities of dissolved carbonate ions. Redistribution of carbonate species, i.e., $CO_3^{2-}$, $HCO_3^-$, $H_2CO_3$, and $CO_2$(aq), occur when $CO_3^{2-}$ is released into solution from cerrusite dissolution and may take minutes to reach steady state (*28*). Therefore, in a kinetic study using a time scale of minutes as the sampling interval, the activity of individual species of the carbonate species cannot be easily determined.

Dissolution of hydroxyapatite in the pH range of 4−7 as a function of time is presented in Figure 2. The dissolution was inversely related to pH. Below pH 4, the dissolution was too rapid to be accurately determined under these experimental conditions. At higher pH values, e.g., pH 6 and 7, the dissolved Ca and $PO_4$ reached steady state and did not change after 60-min reaction. From these measurements, approximately 1 and 4% of the total added apatite was dissolved at pH 7 and pH 6, respectively, within 60 min. In comparison, approximately 20 and 40% of the added apatite was dissolved at pH 5 and pH 4, respectively, after only 25 min. The soluble species compositions at pH 4, 5, and even 6 were stoichiometric to the elemental composition of apatite with a P/Ca molar ratio of 3/5 (Figure 2). However, the $PO_4$ and Ca concentrations at pH 7 were essentially the same. This may be attributed to adsorption of $Ca^{2+}$ because the high pH and the high total surface area of the undissolved apatite are favorable for removal of the cation from solution.

**Reaction of Cerrusite with Hydroxyapatite.** The precipitation of pyromorphite in a saturated solution is a rapid process and is completed within seconds. Therefore, the overall reaction in the cerrusite and apatite system should be kinetically controlled by the dissolution rates of cerrusite or apatite:

$$5PbCO_3(s) + Ca_5(PO_4)_3OH(s) + Cl^-(aq) = Pb_5(PO_4)_3Cl(s) + 5Ca^{2+}(aq) + 5CO_3^{2-}(aq) + OH^-(aq) \quad (1)$$

From eq 1, the soluble Ca can be used as the indicator for the dissolution of apatite because under these conditions there was no reaction to remove the dissolved Ca from the aqueous phase. When the amount of apatite dissolved and the soluble $PO_4$ concentration is determined, the formation of chloropyromorphite can be estimated from the $PO_4$ mass balance assuming that chloropyromorphite formation is the only processes to remove the soluble $PO_4$. From the results of the XRD analysis of this study as well as previous studies (*10*), the formation of chloropyromorphite is the only process in the system that removes soluble Pb and $PO_4$. It is also apparent from eq 1 that the concentrations of soluble Pb or $PO_4$ were determined by either the originally added minerals, e.g., apatite and cerrusite, or the newly formed mineral during the transformation process. If the relative rate of dissolution of apatite is lower than that of dissolution of cerrusite, the soluble Pb will be dependent upon the solubility of cerrusite [$-\log K_{sp} = 13.11$ (*29*)]. As stated before, the soluble Pb level is of interest for its high reactivity and bioavailability. As both cerrusite and apatite dissolution are pH-dependent, the reaction rate of cerrusite and hydroxyapatite should be directly associated with pH.

**pH-Constant Study.** In the experiment with a P/Pb ratio of 3/5, $2.3 \times 10^{-3}$ mol of $PO_4$ as hydroxyapatite together with 1.00 g of cerrusite ($3.74 \times 10^{-3}$ mol of Pb) was placed into a solution and reacted for 60 min under constant pH conditions. The amount of $PO_4$ added was stoichoimetrically equal to that needed to transform the added cerrusite-Pb into chloropyromorphite.

The soluble Ca concentration indicates that nearly complete dissolution of added hydroxyapatite was achieved at pH 2 and pH 3 within 5 min (Figure 3a). At pH 4, about 70% of the apatite was dissolved in 15 min, and 90% of added apatite was dissolved at 60 min. However, apatite dissolution was much lower when the pH value in the solution was above 4; only 55, 15, and 10% of the added apatite was dissolved in the 60-min reaction at pH 5, 6, and 7, respectively (Figure 3a).

The formation rate of chloropyromorphite in the suspensions was proportional to the dissolution of apatite. The XRD patterns indicate that at pH 2 and pH 3 the only mineral in the solid collected after 60-min reaction was chloropyro-

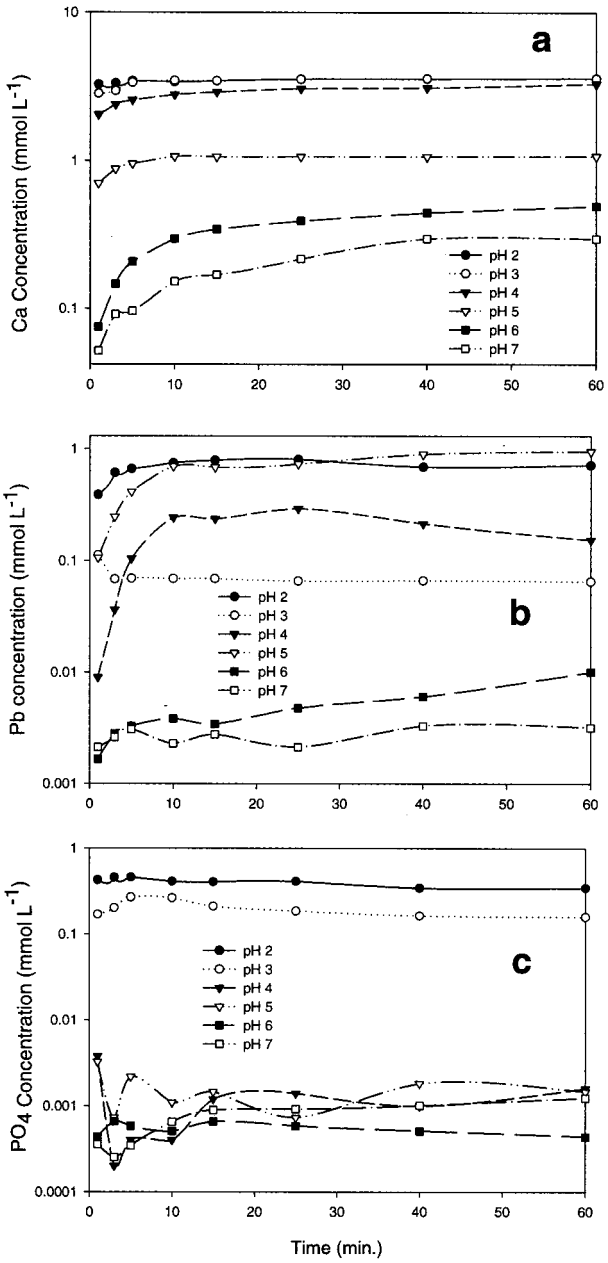


**FIGURE 3. Soluble Ca (a), Pb (b), and $PO_4$ (c) concentrations in the cerrusite–apatite suspensions at various pH values. The P/Pb ratio = 3/5 and *I* = 0.100 M.**

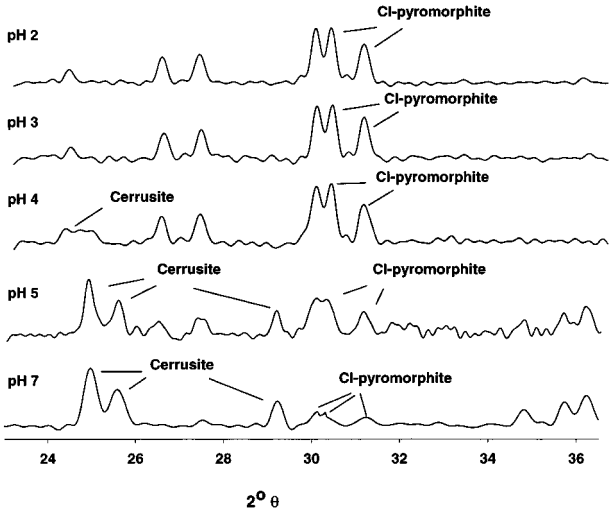


**FIGURE 4. Effect of pH on the transformation of Pb from cerrusite to chloropyromorphite, Reaction time = 60 min, P/Pb ratio = 3/5.**

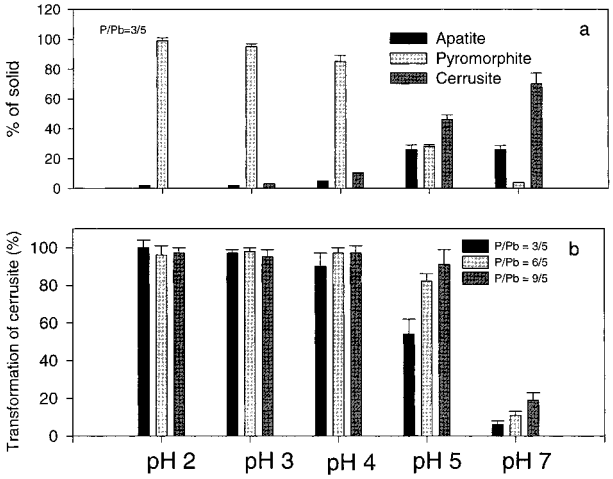


**FIGURE 5. Mineral composition of the solid collected after 60-min reaction (a) and the transformation of cerrusite-Pb to chloropyromorphite-Pb (b).**

morphite (Figure 4). At pH 4, a fingerprint of cerrusite was observed in the XRD pattern, but the dominant mineral was chloropyromorphite. The solid collected at pH 5 after 60 min was a mixture of cerrusite and newly precipitated chloropyromorphite as identified by XRD (Figure 4). The undissolved cerrusite was the dominant mineral in the solid of pH 7, but characteristic peaks of chloropyromorphite were also observed in the XRD patterns. Thus, the added cerrusite was partially transformed into chloropyromorphite at pH 7 (Figure 4).

To quantify the transformation of cerrusite-Pb into chloropyromorphite-Pb, the total $PO_4$, Ca, and Pb contents of the collected solids were determined, and the mineral composition in these solids were calculated. At pH 2, 3, and 4, there were essentially no cerrusite in the solids (Figure 5a). At pH 5 and above, the cerrusite was a significant constituent of the solid (Figure 5a). These results were consistent with the XRD analysis, which illustrates that the transformation of cerrusite-Pb to chloropyromorphite decreased with increasing pH (Figures 4 and 5a). In terms of the transformation rate, as illustrated in Figure 5b, nearly 100% conversion of cerrusite-Pb to chloropyromorphite-Pb was achieved at pH 2, 3, and 4 regardless of the P/Pb ratio because of the rapid dissolution of cerrusite and apatite at low pH conditions. In contrast, when the solution pH was greater than 5, the transformation rate was increased with increasing P/Pb ratio (Figure 5b). This may be attributed to the rate of apatite dissolution, which is proportional to the total surface area of solid apatite in the suspension.

The estimated soluble Pb levels from the solubility of chloropyromorphite [$-\log K_{sp} = 84.4$ (*30*)], $10^{-3.50}$ and $10^{-4.34}$ M, at pH 2 and pH 3, respectively, were in general agreement with the measured soluble Pb concentrations, $10^{-3.1}$ and $10^{-4.15}$ M (Figure 3b), implying that chloropyromorphite was controlling Pb concentration in solution. This indicates that only chloropyromorphite-Pb was present and is in agreement with the XRD analysis of the solids (Figure 4).

Considering the soluble $PO_4$ concentration of $10^{-5.28}$ M at pH 4, the concentration of soluble Pb should be $10^{-4.8}$ M if it was controlled by dissolution of chloropyromorphite. However, the measured soluble Pb at pH 4 was $10^{-3.62}$ M (Figure 3b), which was 1 order of magnitude higher than that estimated from the solubility of chloropyromorphite, but about 1 order of magnitude lower than that of the suspension containing only cerrusite (Figure 1). This observation implies

that the trace amount of cerrusite that remained in the suspension of pH 4 still played a role in determining the soluble Pb concentration even though nearly all of the added Pb had been converted into chloropyromorphite. At pH 5, the soluble Pb was $10^{-3.04}$ M (Figure 3b), which was comparable with the concentration obtained from the suspension containing only cerrusite, $10^{-2.95}$ M (Figure 1). As illustrated in Figure 4, approximately 55% of the added cerrusite-Pb was transformed into chloropyromorphite at pH 5; the soluble Pb level was determined by cerrusite, implying that there was insufficient $PO_4$ ($10^{-6}$ M) to react with Pb to form chloropyromorphite. From Figures 1 and 2, it can be seen that a decrease in dissolution rate of cerrusite from pH 4 to pH 5 was not as significant as that of the decrease in apatite dissolution rate. This indicates that the relative dissolution rate of apatite is lower than that of cerrusite at pH 5 and thus the supply of soluble $PO_4$ is insufficient to precipitate dissolved Pb at this pH. The soluble Pb concentrations at pH 6 and pH 7 were $10^{-5}$ and $10^{-5.5}$ M at 60 min, respectively, about 1 order of magnitude lower than that without apatite, $10^{-3.6}$ and $10^{-4.5}$ M for pH 6 and pH 7 (Figure 1). This reduction in the soluble Pb concentration at these pH values could be attributed to the removal of dissolved Pb by the ongoing reactions, including dissolution of apatite and cerrusite and precipitation of chloropyromorphite. Because the dissolution rate of cerrusite at pH 6 and above decreased dramatically (Figure 1), the rate of $PO_4$ release from apatite dissolution maintained a soluble $PO_4$ level of $10^{-6}$ M (Figure 3c), which provided sufficient phosphate to precipitate the dissolved Pb at this pH level. Thus, the concentrations of soluble Pb were determined by both cerrusite and chloropyromorphite in the suspensions of pH 6 and pH 7.

Although not shown, similar phenomena were observed in the reactions with P/Pb ratios of 6/5 and 9/5. The amount of chloropyromorphite formed in the solid after 60-min reaction decreased with an increase in pH. The total transformation of Pb from cerrusite to chloropyromorphite for the three P/Pb ratios after 60 min under constant pH illustrates that complete transformation is obtained at pH 2, 3, and 4 (Figure 5b). At pH 5 and above, transformation decreased with increasing pH. Increasing the P/Pb ratio caused an increase in the percent of Pb transformed into chloropyromorphite at pH 5 and pH 7 (Figure 5b).

**Effect of Reaction Time**. To test the effect of reaction time on the transformation of Pb from cerrusite to chloropyromorphite, the reactions at pH 6 for each of the three P/Pb ratio experiments were allowed to continue for 48 h instead of 60 min as reported above. The mineral composition of the solids collected after 48 h demonstrated that 83 (±4), 94 (±4), and 96 (±6)% of cerrusite-Pb was converted into chloropyromorphite when the P/Pb molar ratios were 3/5, 6/5, and 9/5, respectively. If we assume that the transformation rate at pH 6 should be between those obtained at pH 5 and pH 7 for a 60-min reaction time (Figure 5b), then the higher transformation rate may be attributed to the longer time of reaction. The XRD patterns for the solids collected for the three P/Pb ratio after 48-h reaction indicate that some of the added cerrusite still remained at P/Pb ratios of 3/5 and 6/5, but it was not shown in the solids collected when the P/Pb ratio was 9/5 (Figure 6). Furthermore, the XRD patterns in Figure 6 also demonstrated that chloropyromorphite mineral was the only reaction product.

**pH-Dynamic Study**. As demonstrated by the soluble Ca concentration (Figure 7), under the condition of variable pH system (initial pH of 2.1−2.4), the added apatite was completely dissolved during the initial 5-min reaction time. The soluble Ca concentration of $3.4 \times 10^{-3}$ M was the result of complete dissolution of the added apatite (0.38 g) that contained $3.78 \times 10^{-3}$ mol of Ca. However, the dissolved $PO_4$

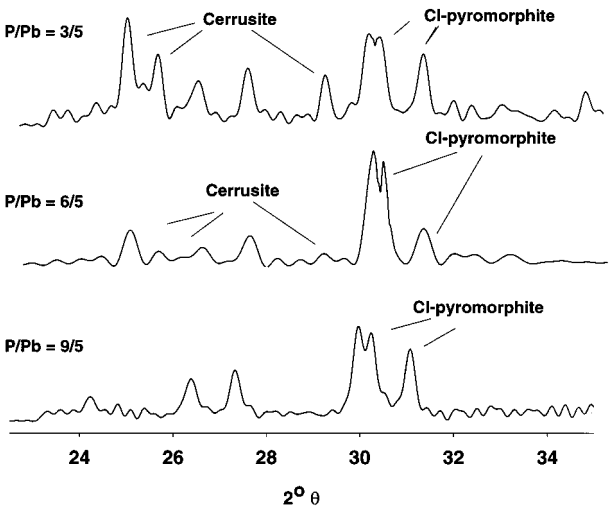


**FIGURE 6. Effect of P/Pb ratios on the transformation of Pb from cerrusite to chloropyromorphite, Reaction time = 48 h, pH = 6.**

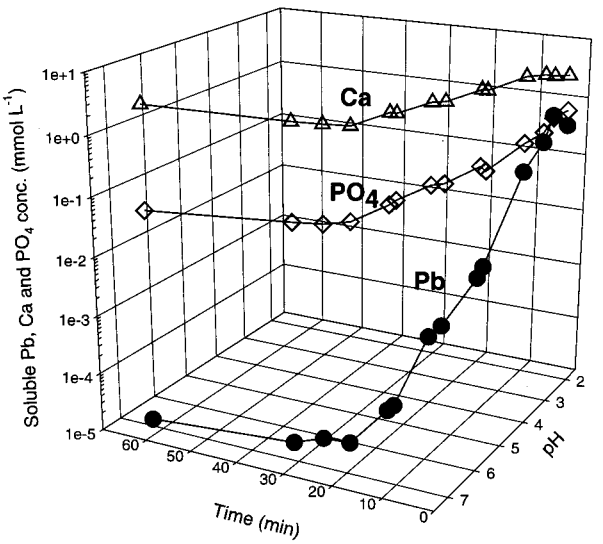


**FIGURE 7. Concentrations of soluble species in cerrusite−apatite suspension as a function of pH and time. The suspension pH was adjusted from 2 to 7 within 20 min, and the total reaction time was 60 min.**

concentration was $3.5 \times 10^{-4}$ M, about 15% of the total $PO_4$ from apatite dissolution. The soluble Pb concentration shown in Figure 7 was $2.4 \times 10^{-4}$ M, about 13% of the Pb added as cerrusite. Considering full dissolution of both apatite and cerrusite at these low pH values and the nearly stoichoimetric removal of Pb and $PO_4$, it can be surmised that chloropyromorphite formation was occurring. This formation of chloropyromorphite was confirmed by the XRD analysis of the solid collected at the end of the experiment (not shown). The transformation of Pb from cerrusite to chloropyromorphite as a function of time was calculated based on the mass balance of $PO_4$, Ca, and Pb in the system. In the pH-dynamic system, more than 95% of added Pb was converted from cerrusite into chloropyromorphite within 10 min and remained in the suspension regardless of the reaction time and increase in pH.

The soluble $PO_4$ level was maintained at $1.0-2.7 \times 10^{-4}$ M after the first 5-min reaction, and this relatively high soluble $PO_4$ level resulted in a low soluble Pb concentration during the reaction (Figure 7). The soluble Pb level was $10^{-5}$ M after 7-min reaction at pH 2.8. This is compatible with that obtained in the pH-constant study (Figure 3b). When the pH was raised to 4.1, after 10-min reaction, the soluble Pb

concentration was $10^{-5.57}$ M, which is about 2 orders of magnitude lower than that from the pH-constant study and agreed with the value, $10^{-5.5}$ M, calculated from the solubility product of chloropyromorphite. The soluble Pb concentration was further decreased to $10^{-6.27}$ M at pH 5, compared to $10^{-3.04}$ M in the pH-constant study. When the suspension pH was raised to 6 and 7, the soluble Pb ranged from $10^{-7.23}$ to $10^{-7.7}$ M, or 10−4 $\mu$g of Pb $L^{-1}$, which is consistent with the solubility of chloropyromorphite and more than 2 orders of magnitude lower than that of the pH-constant study (Figure 3b). Thus, in the pH-dynamic system the solubility of chloropyromorphite controlled the soluble Pb level during the entire reaction process.

Unlike the pH-constant system in which the transformation of Pb from cerrusite to chloropyromorphite was incomplete at pH 4 and above (Figures 2, 4, and 5), in the pH-dynamic suspension the cerrusite-Pb was rapidly and fully converted into chloropyromorphite as long as the amount of phosphate as apatite was stoichiometrically equal to that needed to transform the added Pb in cerrusite into chloropyromorphite.

In the constant pH system, both the undissolved cerrusite and the newly formed chloropyromorphite controlled the soluble Pb levels at pH 4 and above. However, in the pH-dynamic system, the soluble Pb level was determined by chloropyromorphite during the entire reaction period. The complete dissolution of apatite and cerrusite in the initial acidic condition resulted in a high soluble $PO_4$ level that precipitated the soluble Pb from the cerrusite dissolution. This resulted in a rapid precipitation of chloropyromorphite as well as a dramatic reduction of soluble Pb level during the reaction. At pH 4, 5, 6, and 7, the soluble Pb concentrations were $2.4 \times 10^{-4}$, $9.5 \times 10^{-4}$, $1.0 \times 10^{-5}$, and $3.1 \times 10^{-6}$ M in the pH-Constant suspensions, as compared to $2.7 \times 10^{-6}$, $5.3 \times 10^{-7}$, $5.0 \times 10^{-8}$, and $1.9 \times 10^{-8}$ M in the pH-dynamic system. Thus, the soluble Pb was at 10 $\mu$g $L^{-1}$ or lower when pH 6 was reached, which took about 16 min in the pH-dynamic system.

These data demonstrated that the formation of chloropyromorphite from cerrusite and apatite can take place in the pH conditions of the aqueous system of the GI tract. Apparently, under the pH condition of the GI tract, the formation of chloropyromorphite is kinetically favored. Furthermore, the results from constant pH systems cannot predict the Pb−$PO_4$ reaction products obtained in a dynamic pH system because of the reaction kinetics.

In the case where cerrusite is ingested with contaminated soil in the presence of stoichiometric amounts of phosphate(s), it is logical to assume that the soluble Pb concentration will be controlled by the solubility of chloropyromorphite, which is lower than 10 $\mu$g $L^{-1}$ when pH 7 is reached. Thus, one can predict that the bioavailability of Pb from ingested cerrusite would be significantly reduced in the presence of apatite.

## Acknowledgments

We thank Dr. M. Schock of the U.S. EPA for his assistance in XRD analysis. This research was supported in part by an appointment to the Postgraduate Research Participation Program at the National Risk Management Laboratory administrated by the Oak Ridge Institute for Science and Education through an interagency agreement between the U.S. Department of Energy and the U.S. Environmental Protection Agency. Although the research in this paper was undertaken by the U.S. Environmental Protection Agency, it does not necessarily reflect the views of the Agency. Mention of trade names or commercial products does not constitute endorsement or recommendation for use.

## Literature Cited

(1) Ma, Q. Y.; Traina, S. J.; Logan, T. J.; Ryan, J. A. *Environ. Sci. Technol.* **1993**, *27*, 1803−1810.
(2) Ma, Q. Y.; Traina, S. J.; Logan, T. J.; Ryan, J. A. *Environ. Sci. Technol.* **1994**, *28*, 408−418.
(3) Ma, Q. Y.; Traina, S. J.; Logan, T. J.; Ryan, J. A. *Environ. Sci. Technol.* **1994**, *28*, 1219−1228.
(4) Ma, Q. Y.; Logan, T. J.; Traina, S. J. *Environ. Sci. Technol.* **1995**, *29*, 1118−1126.
(5) Ma, L. Q. *J. Environ. Qual.* **1996**, *25*, 1420−1429.
(6) Cotter-Howells, J.; Caporn, S. *Appl. Geochem.* **1996**, *11*, 335−342.
(7) Chowdhury, A. K.; Stanforth, R. R.; Warren, R. S. The 6th IEC Special Symposium on Emerging Technology for Hazardous Waste Management, Atlanta, GA, 1994; American Chemical Society: Washington, DC, 1994; pp 1226−1229.
(8) Xu, Y.; Schwartz, F. W. *J. Contam. Hydrol.***1994**, *15*, 187−206.
(9) Zhang, P.-C.; Ryan, J. A., Soil Science Society of America Annual Meeting, St. Louis, MO, 1995; ASA SSSA: Washington, DC, 1995; p 41.
(10) Zhang, P.; Ryan, J. A.; Bryndzia, L. T. *Environ. Sci. Technol.* **1997**, *31*, 2673−2678.
(11) Ruby, M. V.; Davis, A.; Nicholson, A. *Environ. Sci. Technol.* **1994**, *28*, 646−654.
(12) Cotter-Howells, J.; Cahmpness, P. E.; Charnock, J. M.; Pattrick, R. A. D. *Eur. J. Soil Sci.* **1994**, *45*, 393−402.
(13) Cotter-Howells, J. *Environ. Pollut.* **1995**, *90*, 1−8.
(14) Laperche, V.; Traina, S. J.; Gaddam, P.; Logan, T. J. *Environ. Sci. Technol.* **1996**, *30*, 3321−3326.
(15) Dieter, M. P.; Mathews, H. B.; Jeffcoat, R. A.; Moseman, R. F. *J. Toxicol. Environ. Health* **1993**. *39*, 79−93.
(16) Medlin, E. A. M.S. Thesis. University of Colorado. Boulder, CO, 1995.
(17) Ruby, M. V.; Davis, A.; Link, T. E.; Schoof, R.; Chaney, R. L.; Freeman, G. B.; Bergstrom, P. *Environ. Sci. Technol.* **1993**, *27*, 2870−2877.
(18) Ruby, M. V.; Schoof, R.; Eberle, S.; Sellstone, C. M. *Environ. Sci. Technol.* **1996**, *30*, 422−430.
(19) Gasser, U. G.; Walker, W. J.; Dahlgren, R. A.; Borch, R. S.; Burau, R. G. *Environ. Sci. Technol.* **1996**, *30*, 761−789.
(20) Logan, T. J.; Traina, S. J. In *Metals in Groundwater*; Allen, H. E., Perdue, E. M., Brown, D. S., Eds.; Lewis Publishers: Ann Arbor, MI, 1993; pp 309−347.
(21) Nriagu, J. O. *Inorg. Chem.* **1972**, *11*, 2499−2503.
(22) Evans, E.; Ma, M.; Kingston, L.; Leharne, S.; Chowdhry, B. *Environ. Int.* **1992**, *18*, 153−162.
(23) Harrison, R. M. *Environ. Sci. Technol.* **1981**, *15*, 1378−1384.
(24) Krishanmurthy, S. *Environ. Prog.* **1993**, *11*, 256−260.
(25) Morrison, G. M. P. In *Speciation of Metals in Water, Sediment and Soil Systems*; Landner, L., Ed.; Springer-Verlag: New York, 1987; Vol. 11, p 63.
(26) Xian, X. *Plant Soil* **1989**, *113*, 257−264.
(27) Chlopecka, A. *Water Air Soil Pollut.* **1996**, *87*, 297−309.
(28) Stumm, W.; Morgan, J. J. *Aquatic Chemistry*, 2nd ed.; John Wiley & Sons: New York, 1981.
(29) Schock, M. R. *J. Am. Water Works Assoc.* **1980**, *72*, 695−704.
(30) Nriagu, J. O.; Moore, P. B. *Phosphate Minerals*; Springer-Verlag: New York, 1983.

*Received for review March 17, 1998. Revised manuscript received November 4, 1998. Accepted November 4, 1998.*

ES980268E